Improving the efficiency and performance of low-temperature combustion with thick thermal barrier coatings

Ziming Yan, Brian Gainey, James Gohn, Deivanayagam Hariharan, John Saputo, Carl Schmidt, Felipe Caliari, Sanjay Sampath, Benjamin Lawler

Abstract

Thick thermal barrier coatings (TBCs) have a significant potential to increase thermal efficiency by reducing heat transfer losses. However, in conventional combustion modes, the drawbacks associated with charge heating and higher propensity to knock have outweighed the efficiency benefits. Since the advanced low-temperature combustion (LTC) concepts are fundamentally different from the conventional combustion modes, these penalties do not exist in most of LTCs.

The current experimental study shows the feasibility and benefits of thick TBCs with advanced LTC enabled by two different fuels: conventional gasoline and wet ethanol 80 (WE80, i.e., 80% ethanol and 20% water by mass). A total of five pistons were tested, including two metal baselines and three TBC-coated pistons with different thicknesses or surface finishes. A load sweep was conducted with each fuel on each piston within the same constraints. The thick TBCs extends the low load limit by about 15% for both gasoline and WE80 cases. A deterioration of the high load limit was not observed, which implies that the charge heating penalty does not occur in LTCs. The combustion efficiency increased for the thicker TBC by up to 2 percentage points, and the thermal efficiency was increased by up to 4.3%. The gasoline cases experience the largest benefits at low load, while the wet ethanol experiences the largest benefits at mid-to-high load. The intake temperature requirement is successfully reduced by 10 to 15 K. It is also observed that the dense sealing layer results in a significant improvement to UHC emissions. All of the coated pistons survived the 10 to 20 hours of engine operation with no visual failure.

Introduction

Thick Thermal Barrier Coatings (TBCs) with advanced Low-Temperature Combustion (LTC)

Thick TBCs have been tested in the past with conventional combustion modes such as spark ignition (SI) and conventional diesel combustion. Although these past studies were able to achieve modest efficiency gains and prove the experimental feasibility of ceramic coatings in internal combustion engines, there were several unforeseen problems. For example, one of the issues that was discovered was that a large amount of heat transfer losses that were saved by the TBC were converted into higher exhaust losses instead of into useful work [1]. However, a more significant concern was that with thick TBCs, the wall temperatures during the intake stroke increased, which led to a large amount of charge heating during the intake stroke. This charge heating reduced the density of incoming charge and reduced the peak power density of the engine [2]. Furthermore, there was also a considerable challenge with SI engines where the hot walls with thick TBCs lead to engine knock [3]. For these reasons, the community shifted focus from thick TBCs to thin, “temperature swing” coatings. Ideally, these thin temperature swing coatings allow a dynamic response of the surface temperature [4]. During the intake stroke, the surface temperature will be cooled immediately by the intake charge to minimize intake charge heating, and during compression, combustion, and expansion, the surface temperature will be rapidly elevated to reduce heat transfer from the trapped charge [5]. This approach is promising, but also heavily relies on a specific set of material properties, such as a very low thermal conductivity paired with minimal heat capacity and density [4]. The current state-of-the-art coating techniques are not yet able to implement such coating materials into internal combustion engines without compromising strength and durability, especially in the harsh environment of the combustion chamber of an engine.

The first attempts of thick coatings occurred in the 80s [6][7][8]. Since then, advanced combustion concepts, specifically low-temperature combustion (LTC) modes, have been proposed, developed, and further studied. The combustion (i.e., heat release process) of these LTC concepts is fundamentally different from SI and conventional diesel combustion [9][10][11]. The majority of these LTC modes require a relatively high intake valve closing (IVC) temperatures to enable autoignition, and that is usually achieved by trapping hot residuals or increasing intake temperature. Kuo et al. showed the feasibility of using a flexible valvetrain with negative valve overlap to increase internal residuals; however, the penalty associated with extra pumping losses was also noticeable [12]. Whether a particular LTC strategy achieves autoignition with internal hot residuals or with direct intake heating, LTC incurs a significant charge heating penalty to achieve autoignition, which is associated with a loss of power density. In which case, applying thick TBCs with LTC modes does not incur any additional charge heating penalty beyond what is needed to achieve autoignition, and therefore, thick TBCs in LTC do not have the same drawbacks encountered in the past for conventional combustion modes.

In recent years, with continuing research and development of LTCs, the operable load range had been improved significantly [13][14][15]. Based on the understanding of homogeneous charge compression ignition (HCCI), many second-generation LTC concepts have been proposed that are able to extend the high load limit by staggering the heat release process via different mechanisms. For example, the staged ignition of reactivity controlled compression ignition (RCCI) is based on the in-cylinder reactivity gradient [16][17]; the trigger of low-temperature gasoline combustion (LTGC) including partial fuel stratification (PFS) and gasoline compression ignition (GCI) is based on φ-stratification and mixing controlled mechanisms, respectively [18][19][20]; the sequence of ignition in thermally stratified compression ignition (TSCI) is driven by the in-cylinder temperature distribution [21][22]. Although these LTC strategies still may not be able to achieve loads as high as the state-of-the-art conventional combustion modes yet, the community is still actively working to further extend their load ranges, and the issues of poor control and narrow load range are not as limiting as they previously were.

Although combustion control and the operating range of LTC have improved significantly with second-generation advanced combustion modes, there are still other remaining challenges for LTCs. In addition to requiring high intake temperatures, one of the common challenges with LTC is low combustion efficiency and high unburned hydrocarbon (UHC) and CO emissions. This is mostly due to incomplete combustion happening in the cold regions near the walls and crevices [23]. Another disadvantage of LTC is its low exhaust enthalpy due to the relatively high compression ratios, lean operation, and high thermal efficiency, which is a challenge for aftertreatment and turbocharging. All of the remaining issues with LTC (i.e., high required intake temperature, low combustion efficiency, and low exhaust enthalpies) can be improved with thick TBCs. Thick TBCs will lower the required intake temperature, increase the temperature in

the near-wall areas that contribute to UHC and CO and improve combustion efficiency, and increase exhaust temperature for LTC aftertreatment and turbocharging. Therefore, there is a promising marriage between the thick TBCs and the LTC, which can result in high brake efficiencies without any additional charge heating penalty and while mitigating the remaining issues of LTC.

Wet Ethanol (WE) – an Alternative Biofuel

Tightening CO_2 emissions regulations have inspired the engine research community to seek low-carbon solutions to the transportation needs of society. One of these approaches is to increase engine efficiency and simultaneously decrease emissions, which has been demonstrated with advanced combustion modes such as LTC described above. A parallel and additive approach is the production and use of alternative, low-carbon or net-carbon-neutral, fuels such as biofuels and e-fuels, which can considerably reduce CO_2 emissions from a lifecycle perspective [24].

Ethanol is the most extensively used and mass-produced biofuel in the United States [25] and possibly the world. Since ethanol is currently added to commercial gasoline, the water content must be removed during the ethanol production process to ensure miscibility with gasoline. There are three steps in the production of neat ethanol (i.e., 100% ethanol): the fermentation of a sugar or starch (usually sugarcane in Brazil or corn in the U.S.), the distillation process, and the dehydration process. The energy consumption during the distillation and dehydration processes account for up to 37% of the total energy required to produce neat ethanol [26]. Additionally, the required distillation energy becomes extremely non-linear when the ethanol percentage surpasses 80%. Therefore, a considerable amount of energy can be saved if the engine can make use of an ethanol-water mixture, which is called wet ethanol or hydrous ethanol, where WE80 corresponds to a mixture of 80% ethanol and 20% water.

Compared with other fuels such as gasoline and diesel, the ethanol itself has a very high latent heat of vaporization. Adding water further increases the heat of vaporization of the mixture, which presents unique opportunities but also challenges. This extremely high cooling potential gives wet ethanol the ability to control the IVC temperature by varying the injection timing during the intake stroke, which varied the fraction of heat that was absorbed from the combustion chamber surfaces versus the incoming charge [27]. This result means that cycle-to-cycle control over combustion phasing in LTC can be achieved by varying the intake stroke injection timing of wet ethanol [27]. When an injection event occurs during the compression stroke, the evaporative cooling amplifies thermal stratification, which staggers the ignition timing of various regions and results in a significant load range extension [28]. However, this massive evaporative cooling capacity further increases the intake temperature requirement of LTC to balance the cooling effect from vaporization. Additionally, the wet ethanol can result in increased wall wetting because of its cooling potential. By applying thick TBCs with LTC of wet ethanol, the charge heating penalty incurred by the TBCs can be used to counteract the intake evaporative cooling, and the thick TBC can provide hotter walls that ensure proper evaporation. Thus, it is mutually beneficial to use thick TBCs with wet ethanol advanced LTC.

A previous experimental study demonstrated the feasibility of using thick TBCs with wet ethanol LTC and characterized some of the gains associated with the combination of the thick TBCs, wet ethanol, and LTC [29]. However, the performance of thick TBCs at different loads, including the impact on the high load limit, as well as an evaluation of the TBCs' performance with a conventional fuel such as gasoline in comparison to wet ethanol, has not been systematically explored and studied. Therefore, the motivation of this study is:

1. ***To evaluate the effects of thick TBCs on LTC, energy distribution, and emissions at different load conditions***

2. ***To comprehensively compare the potential benefits of thick TBCs with two different fuels: conventional gasoline and WE80***

Experimental Setup and Methodology

First, the engine test cell setup and the methodology of the heat release analysis will be introduced. Then, the coatings properties, the preparation process, and the plasma thermal spray technology will be provided.

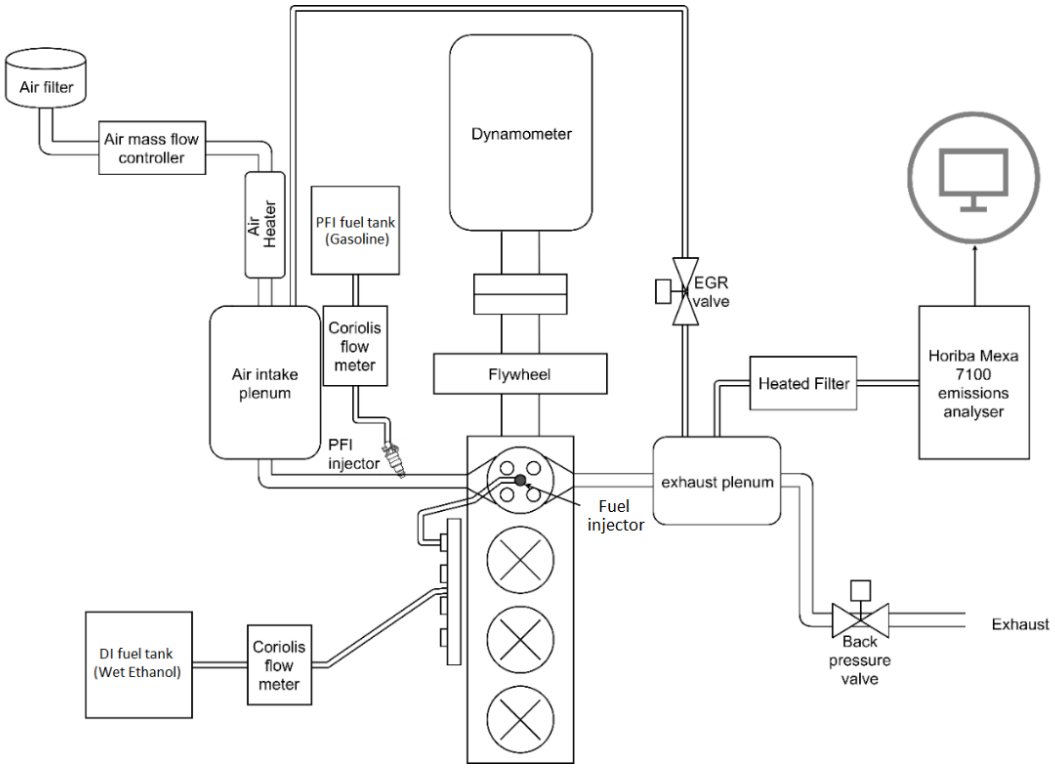

Figure 1: Engine test cell layout

Experimental Engine Test Cell

The experiments were conducted on a 421.5 cc single-cylinder light-duty diesel engine. Figure 1 shows the layout of the entire engine system. The Ricardo Hydra engine block was coupled with the first cylinder of a production four-cylinder, 1.7-liter GM-Isuzu engine head, and the other cylinders were deactivated. Since advanced combustion modes do not rely on in-cylinder turbulence and mixing in a similar manner to the conventional combustion modes, the OEM piston with a re-entrant bowl piston was replaced by a custom-designed shallow bowl piston (shown in Figure 2) to improve heat transfer characteristics, combustion efficiency, and UHC emissions associated with the LTC. Figure 2 shows the geometry of the combustion chamber with the custom-designed pistons at top dead center (TDC). The custom piston was designed to have the same compression ratio (CR) as the production re-entrant bowl piston. It can be noted that the squish region has been considerably reduced with the shallow bowl design, which helps minimize incomplete combustion. Moreover, the more favorable surface-to-volume ratio could potentially reduce heat transfer losses [30].

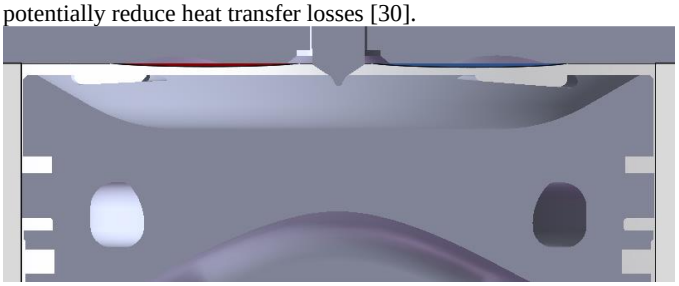

Figure 2: Geometry of the combustion chamber at TDC

Table 1: Engine specifications

Displaced volume	421.5 cc
Stroke	86 mm
Bore	79 mm
Connecting Rod	160 mm
Compression ratio	Targeted at 15.8:1
Number of Valves	4
Exhaust Valve Open	140° ATDC
Inlet Valve Close	-146° ATDC

Additional engine geometric parameters are shown in Table 1. The piston preparation process from the stock piston blank to the final coated piston is shown in Figure 3. First, the blank piston was machined down by a certain depth with the desired shallow bowl geometry. The depth depended on the desired coating thicknesses for different coatings. Then, the primary coating materials were plasma sprayed onto the top surface of the piston, layer-by-layer, while masking the other piston surfaces such as the ring pack area and the piston shirt. The final step depended on whether the dense top sealing layer was desired. If the dense sealcoat was desired, a much denser layer of smaller particles (to reduce or eliminate open pores) of the same material as the primary coating was added onto the surface of the coated piston and some light surface polishing was performed. A more elaborate description of the spray and coating technique is provided in the following section.

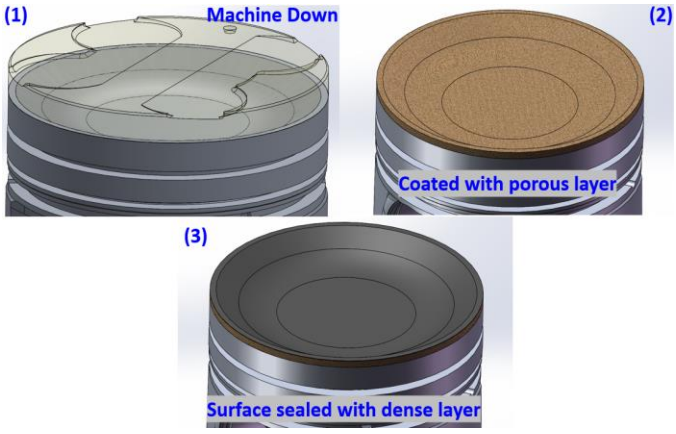

Figure 3: TBC machine & spray process

Two fuels were tested in this study. First, 87-AKI (antiknock index) gasoline is chosen as a conventional fuel that is injected into the intake port to create a homogeneous air-fuel mixture. The gasoline was an EPA Tier III EEE certification gasoline with 10% ethanol from Haltermann Solutions. In addition to gasoline, wet ethanol 80 was chosen as an alternative fuel with a very high latent heat of vaporization, which is 80% ethanol and 20% water on a mass basis. Since this fuel has very high cooling potential, the wet ethanol was direct injected to determine the interactions between the spray impingement of a high heat of vaporization fuel on the hot piston surface. A Bosch CP3 pump pressurized the fuel to 500 bar and then delivered it to the high-pressure production common rail. The injector that was used in the direct injection (DI) system is a centrally mounted, Bosch solenoid-style injector with a 150° included angle. Due to the lubricity difference between wet ethanol or gasoline and diesel, 500 ppm of Infineum R655 lubricity additive was mixed with the fuel by a pneumatic mixer before adding it to the fuel system. It was shown that amount of lubricity additive does not impacts the fuel's reactivity or the heat release process [28]. The fuel properties are listed in Table 2.

Table 2: Fuel properties

Fuel	87-AKI gasoline	Ethanol	WE 80
H/C Ratio	2.003	3	3.64
O/C Ratio	0.0333	0.5	0.82
Ethanol Content [%]	9.9	100	80
Water Content [%]	0	0	20
Lower Heating Valve [MJ/kg]	41.85	26.74	21.39
Anti-knock Index (R+M)/2	87.5	100	-

The intake air was heated by a 5-kW inline heater, which was controlled by a PID controller. The emissions were sampled from the exhaust plenum by a Horiba MEXA 7100 D-EGR emission analyzer via a heated filter and the sample lines. The emissions bench measures five emissions species: the unburned hydrocarbon (UHC), carbon monoxide (CO), carbon dioxide (CO_2), oxygen (O_2), and oxides of nitrogen (NO_x). The intake, exhaust, and the cylinder pressure were measured every 0.1 crank angle degree (CAD), and a Kistler crank angle encoder triggered the pressure measurements.

The measured data were monitored and recorded through a custom Labview program. Some combustion performance features are processed in real-time, including the engine load, thermal and combustion efficiencies, and the heat release characteristics. Data were recorded for 300 consecutive cycles once the engine conditions reached steady state. The recorded data were further processed with a high-fidelity Matlab script that uses the NASA polynomials for mixture properties such as the ratio of the specific heats. The heat transfer losses were determined by the Chang heat transfer correlation developed specifically for LTC [31] and then scaled to match the difference between the fuel energy in the cylinder and the cumulative net heat release by the energy closure method. The gross heat release rate (GHRR) is determined by adding the heat transfer losses and net heat release rate (NHRR). An uncertainty analysis of the heat release process was conducted during post-processing [32].

Table 3 shows the engine operating conditions. The engine was operated naturally aspirated in HCCI with two fuels and five pistons. For each combination of the piston and fuel, a load sweep was performed while maintaining the peak pressure rise rate (PPRR) below ~5 bar/CAD.

Table 3:Engine operating conditions

Engine Speed [rpm]	1200
DI Fuel	Wet Ethanol 80
DI SOI Timing [deg aTDC]	-330
DI Pressure [bar]	500
PFI Fuel	87-AKI Gasoline
PFI SOI Timing [deg aTDC]	-120
PFI Pressure [psi]	28
IMEP [bar]	Swept from 2 bar to 5 bar
Coolant Temperature [K]	370
Oil Temperature [K]	360

The data were recorded after reaching steady-state to ensure the data quality, and the following metrics were indicative of steady-state operation: the variation of CA50 (i.e., the crank angle location where 50% of the mass has burned) was less than 0.5 CAD, the intake temperature variation was less than 0.3 K, and the coefficient of variation (COV) of net IMEP was less than 3%.

Application of the TBCs and Measurements of Their Thermophysical Properties

An argon-hydrogen atmospheric plasma spray (APS) process (Oerlikon Metco, F4MB) configured with a 6mm nozzle and a 90° 1.8mm injector were used to fabricate the primarily yttria-stabilized zirconia (YSZ, Saint Gobain, SG204) TBCs. The piston surfaces were prepared for TBC application by grit blasting the surface at 60 psi from a 125mm distance using 24 mesh alumina grit. The surfaces were then cleaned and dried and were ready for TBC application by APS. Previous attempts to apply thick TBCs (on the millimeter scale) experienced issues of cracking, delamination, or other failures induced by thermal stresses during the engine cycle [33]. It was determined that these issues were related to the difference in the coefficient of thermal expansion (CTE) between the base piston material and the coating which resulted in internal stresses [34]. Additionally, thicker coatings posed a larger challenge because of the larger change in temperature; therefore, the internal stresses increased with the coating thickness. This issue can be resolved by functionally grading the CTE layer-by-layer to minimize the step changes in CTE and reduce thermal stresses [35]. In the present study, four layers of varying composition were applied to grade the CTE starting from pure Ni5Al (Oerlikon Metco, 480NS) as a bond coat applied to the surface of the uncoated piston. This bond coat represented about 5% of the total thickness of the layer and was used to increase adhesion strength and resist high-temperature oxidation in addition to grading CTE. Following the bond coat, a 50-50% by volume YSZ-Ni5Al layer was applied constituting 10% of the total thickness of the coating. Next, a 70-30% by volume layer was sprayed representing 20% of the total thickness. Finally, the bulk (65%) of the thickness of the coating was a 95-5% mixture by volume of YSZ and Ni5Al. If the top sealcoat was desired, then an additional

97-3% by volume thin layer was applied at about 40 µm. The seal coat was comprised of a finer YSZ feedstock (Saint Gobain, SG240F) and a finer Ni5Al (Orelikon Metco, Diamalloy 4008).

A TA Instruments DXF 3050 thermal flash method was used to determine the properties of each layer. An optical micrograph of the unsealed and sealed TBCs layers are shown in Figure 4 and 5, respectively. Table 4 has the details of each layer and . Table 5 has the effective coating properties. Table 6 has the carrier gas flow rates which were optimized based on principles reported by Vasudevan et al. [36] and the plasma gas flow rates and power, which were determined based on a design of experiment considering in-flight particle properties (Tecnar Automation AccuraSpray 3G) as outlined by Vaidya et al. [37]. For more information about the thermal spray process, please refer to [38].

Table 4:Coating layer properties

Layer	L1	L2	L3	L4	L5
1mm Layer Δx [µm]	50	100	200	650	40
2mm Layer Δx [µm]	120	240	480	1560	40
2mm Unsealed Layer Δx [µm]	120	240	480	1560	-
k [W/m-K]	14.2	7.57	4.48	0.93	1.74
ρ [kg/m^3]	7511	5893	5577	4490	5706
c [J/kg-K]	410	309	319	363	442
α [mm^2/s]	4.62	4.15	2.52	0.52	0.69

Table 5: Combine layer properties

Combined Layer	1 mm sealed	2 mm sealed	2 mm unsealed
Thickness [µm]	1040	2440	2400
k [W/m-K]	1.328	1.267	1.261
ρ [kg/m3]	5026	4895	4880
c [J/kg-K]	354.3	347.9	346.0
α [mm2/s]	0.7455	0.7442	0.7469

Table 6: APS configurations

Layer	L1	L2	L3	L4	L5
Argon [NLPM]	45	45	45	45	47
Hydrogen [NLPM]	4	6	6	6	6
Current [A]	550	550	550	550	600
Carrier Gas [NLPM]	3.5	4	3	3.5	3.5
Spray Distance [mm]	100	150	150	150	100

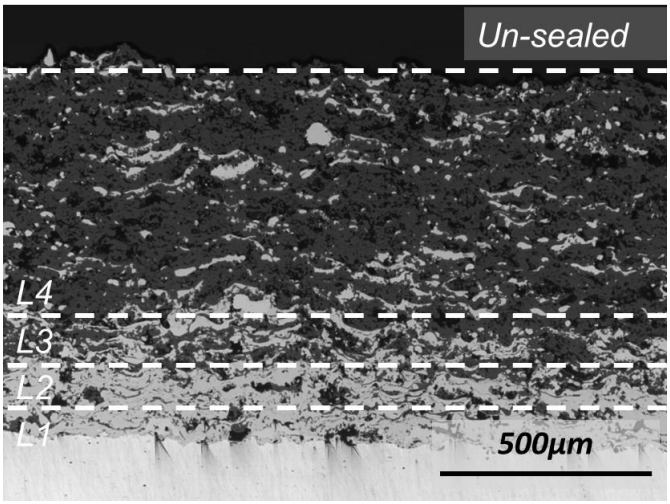

Figure 4: Optical micrographe for unsealed TBC layers

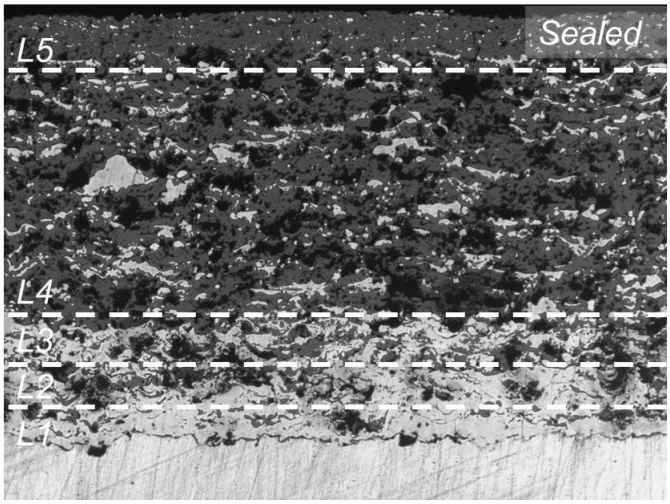

Figure 5: Optical micrograph for sealed TBCs layers

Results and Discussion

The main objective of this study was to investigate the effects of thick TBCs on the combustion and emissions characteristics of LTC. In this study, five pistons were tested, including three coated pistons and two uncoated metal pistons to serve as baseline/reference values. For all of the coated pistons, the desired coating thickness was pre-machined off of the surface of the piston to provide the desired compression ratio to match the metal baseline piston; however, due to the inaccuracies in the machining process, the actual compression ratio of the coated pistons was slightly different from the desired value and ranged from 14.7 to 15.2. In order to provide a thorough comparison, two metal baseline cases were tested with two different thickness head gaskets designed to bracket the range of compression ratios of the coated pistons. The thick head gasket had a compression ratio of 14.0:1, and the thin gasket had a compression ratio of 15.8:1. It can be seen in Figure 6 that three of the coated pistons are grouped relatively close to each other at a compression ratio of ~15.0:1 which is almost perfectly in between the two metal baselines cases. By bracketing the compression ratios in this way, although a perfectly fair direct comparison cannot be made between any one coated piston case and a metal baseline case, when a trend falls outside of the bracket, a strong conclusion can be made that the effect of TBC overpowers the effect of the difference in the compression ratio. Additionally, since the coated pistons are relatively close in compression ratio, direct comparisons can be fairly made between any two coated cases.

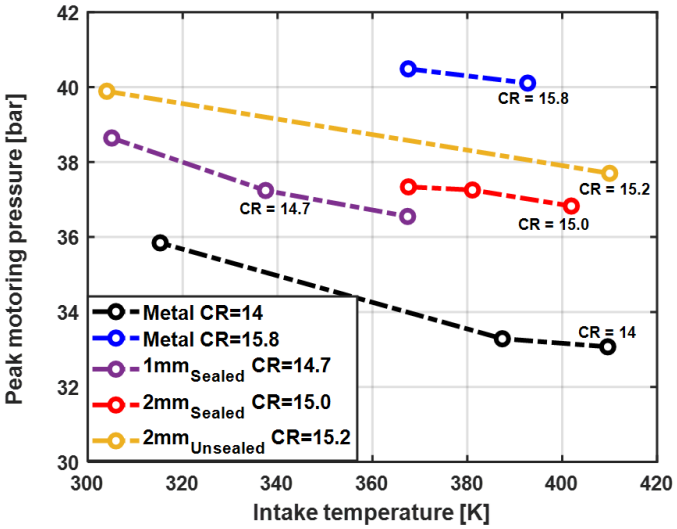

Figure 6: Peak motoring pressure vs. intake temperature

Two fuels were investigated in this study. The gasoline experiments are intended to determine the effects of thick TBC on HCCI combustion with a conventional fuel. Wet ethanol is intended to determine the interactions between thick TBCs and fuels with a high evaporative cooling effect. A load sweep was performed for each fuel and piston combination. During the load sweep, the low load was limited by excessive incomplete combustion and COVs of $IMEP_g$, while the high load was limited by the peak pressure rise rate. In the following sections, the effects of thick TBCs on gasoline HCCI will be illustrated first; then, the assessment of thick TBCs using wet ethanol as fuel will be presented and compared with conventional gasoline.

The Heat Release Process and Load Range – Gasoline

The gross heat release rate (GHRR) and cylinder pressure are shown in Figure 7. The lowest load of approximately 2 bar $IMEP_g$ is shown on the top plot, and the highest load of approximately 4.6 bar $IMEP_g$ is shown in the bottom plot. The pressures after compression and the peak pressures during combustion vary by piston due to the compression ratios differences. More importantly, at a certain load condition, regardless of the coated or metal pistons, the combustion phasings are kept constant, and the heat release profiles are very similar. At the high load condition in the bottom plot, the metal piston with CR = 15.8 (shown in blue) has a lower peak heat release rate; this is presumably due to slightly retarded combustion phasing.

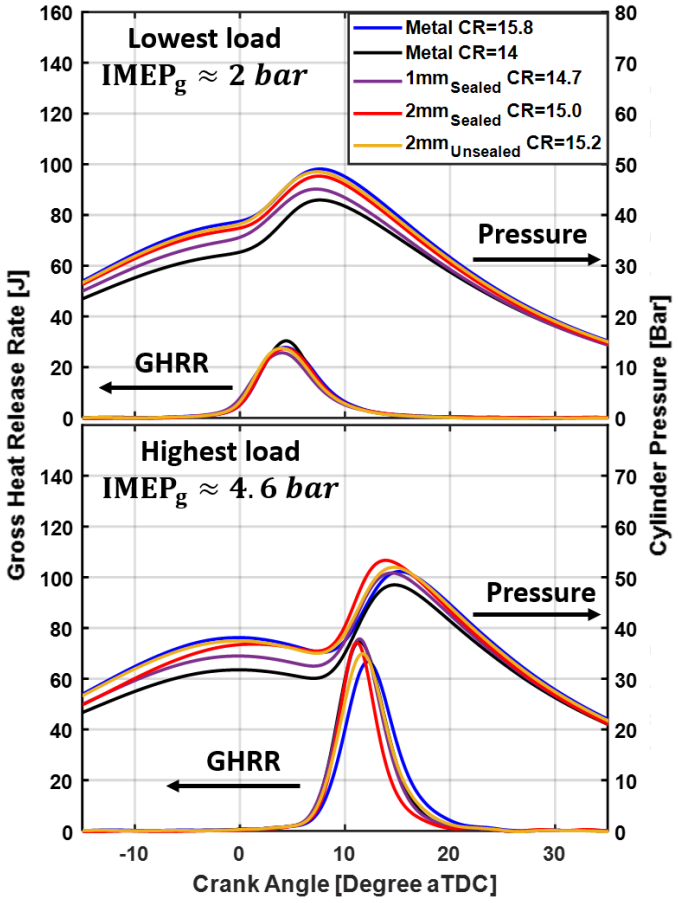

Figure 7: Gross heat release rate (right) & cylinder pressure (left) vs. crank angle

Additional combustion characteristics are shown in Figure 8, including the PPRR, the CA50 combustion phasing, and the 10-90% burn duration. Throughout the load sweep, the combustion phasing of different pistons was kept fairly consistent, and the CA50 is retarded as the load increases because of the threshold of PPRR of ~5 bar/CAD. The PPRR plot in Figure 8(a) and the burn duration plot in Figure 8(c) show that the 2mm sealed TBC piston (red) has the highest PPRR and the shortest burn duration among all of the tested pistons; however, the various piston cases are sometimes mixed with each other and the trends are therefore inconclusive. It was hypothesized that TBCs might reduce the high-load limit of HCCI, since HCCI combustion is extremely sensitive to the wall temperatures and the thermal stratification in the cylinder [39][40], which might indicate that the higher surface temperatures with TBC would accelerate the combustion process. However, the data collected here did not conclusively show any impact of the TBCs on the high-load limit of HCCI, since the 1mm sealed TBC, 2mm unsealed TBC, and two metal baselines show the same trend. Thus, it can be concluded that among all of the tested pistons, the thick TBCs do not have a noticeable impact on the heat release process. This is an important finding because TBCs were shown to affect the high-load limit of both SI and conventional diesel combustion due to charge heating. These results show that this effect is not a consideration for the high-load limit of HCCI.

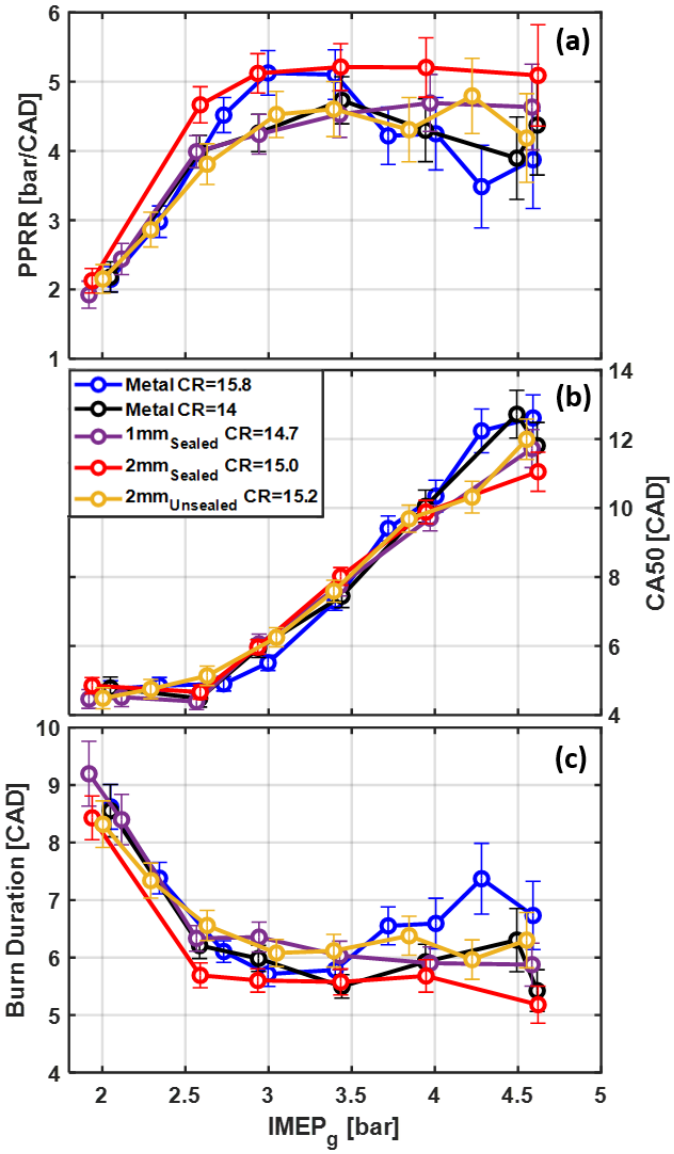

Figure 8: (a) PPRR, (b) CA50 combustion phasing, and (c) 10-90% burn duration vs. $IMEP_g$

Contrary to the high-load limit, the low-load limit is considerably extended by the TBCs. In this study, the low-load limit is defined as the load when combustion efficiency is excessively low (below 86%). As shown in Figure 9, the dashed line is the low-load cutoff line. The metal baselines reach the low load limit of 2.35 bar, and the 2mm TBC case reaches 2 bar which is a 14.8% extension on the low-load limit.

Efficiency and Energy Distribution – Gasoline

This paper follows the efficiency terminology and definitions in Heywood [41]. The combustion efficiency, $\eta_{combustion}$, is defined as the percentage of fuel that burned during the combustion process, and it is calculated from emissions speciation. The gross indicated fuel conversion efficiency, $\eta_{ig,f}$, is the efficiency based on the total fuel energy delivered to the engine. The mathematical definition is shown in the following equation:

$$\eta_{ig,f} = \frac{W_{ig}}{m_{fuel} * Q_{lhv}} \quad (1)$$

where the thermodynamic work in the numerator is calculated from the measured cylinder pressure and volume. The total fuel energy is the denominator where m_{fuel} is the fuel that is delivered to the engine per cycle, and the Q_{lhv} is fuel's lower heating value. Since the fuel that is delivered to the engine does not completely release its energy, the gross indicated thermal efficiency, $\eta_{ig,th}$, is introduced to decouple the effects of unburned fuel on the thermodynamics. The derivation of gross indicated thermal efficiency and the relationship between these three efficiencies is shown in the equation below:

$$\eta_{ig,th} = \frac{W_{ig}}{m_{fuel} * Q_{lhv} * \eta_{combustion}} = \frac{\eta_{ig,f}}{\eta_{combustion}} \quad (2)$$

In this calculation, the denominator only includes the energy that is released from the oxidized fuel because that is the heat that was added to the thermodynamic cycle (i.e., the "thermal" efficiency).

Figure 9 shows all three efficiencies introduced above. It can be seen in Figure 9(a) that the combustion efficiency generally increases with the load due to higher bulk temperatures. The two metal baseline cases are relatively close to each other, with the lower compression ratio case having a slightly higher combustion efficiency. This is due to the higher pressures before ignition for the higher compression ratio case which store more unburned fuel in the crevices. This trend agrees well with the findings from Sjöberg et al. [42]. The combustion efficiency of the TBCs cases is generally higher than that of the metal baseline cases, and the 2mm sealed TBC case has the highest gain of about 1.5 percentage points. For the TBC cases with a top seal coat, the combustion efficiency increases with TBC thickness. Since most of the incomplete combustion in LTCs occurs in the cold regions near the combustion chamber walls, the increased TBC thickness elevates the surface temperature and improves the combustion efficiency. However, the 2mm unsealed case does not show a significant benefit to combustion efficiency, which indicates that the dense sealing surface has a substantial impact on fuel oxidization by sealing open pores which can store unburned fuel. Tree et al. have shown the impacts of piston surface roughness and porosity on fuel consumption of a diesel architecture [43]. Additionally, Hoffman et al. have indicated that the porosity and surface roughness could potentially cause fuel pooling and absorption for open surface pores during HCCI operation [44].

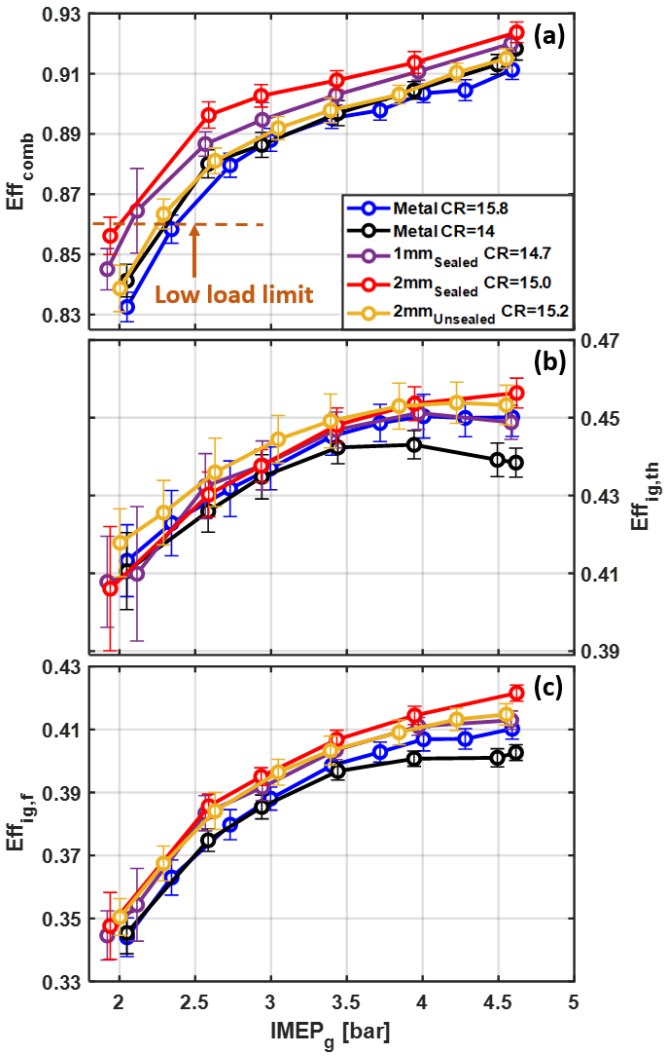

Figure 9: (a) Combustion efficiency, (b) gross indicated thermal efficiency, and (c) gross indicated fuel conversion efficiency vs. $IMEP_g$

Figure 9(b) shows the gross indicated thermal efficiency. As expected, the thermal efficiency of the TBC cases is generally higher than the metal baseline cases, and both two 2 mm TBCs are generally higher than all the other cases. Since the reduction of heat transfer losses and increase in thermal efficiency are only related to the material's properties and the TBC thickness but not the surface porosity, the thicker coatings generally have higher thermal efficiencies than the thinner TBC or metal baselines. The differences between the two metal baseline cases are due to the different CRs, where the higher CR case has a higher thermal efficiency.

In equation (2), the indicated fuel conversion efficiency is the product of the combustion efficiency and the indicated thermal efficiency. As a result, the fuel conversion efficiency of the 2mm sealed TBC case achieves the highest efficiency gain by 1.5 to 2 percentage points, which is about a 4-5% increase due to better combustion efficiency and higher thermal efficiency due to reduced heat transfer losses. The 1mm sealed and the 2mm unsealed cases have approximately the same improvement because the former has higher combustion efficiency and the latter has higher thermal efficiency. The fuel conversion efficiency gain with TBCs appears to have a trend of diminishing returns with increasing thickness, where the increase from metal to 1mm is about 1.5 percentage points, and the increase from 1mm to 2mm is only about 0.5 percentage points. However, more thickness trials are required to determine conclusively.

The energy distribution chart of the highest load (at 4.6 bar) is shown in Figure 10. The entire column corresponds to the fuel energy that is delivered to the engine, which includes four sections: 1) the gross work, 2) the combustion inefficiency, 3) The exhaust wasted heat, and 4) the heat transfer losses (from Chang's heat transfer correlations [31] with energy closure as described above). The heat transfer portions are generally lower for TBC cases, which supports the trends in thermal efficiency and the analysis mentioned above. The saved heat transfer losses and the reduced unburned fuel increase the useful work and the exhaust gas enthalpy. Comparing two metal baselines, the heat transfer losses are approximately the same, and the $Metal_L$ case (the thicker head gasket and lower compression ratio) has higher exhaust enthalpy and lower work output because of the lower compression ratio and lower thermal efficiency. Note that if the compression ratio of metal baseline perfectly matched the TBC cases, the values of the baseline would be about the average of the two metal cases, since the change in compression ratio is small and the trend can be considered linear over that range.

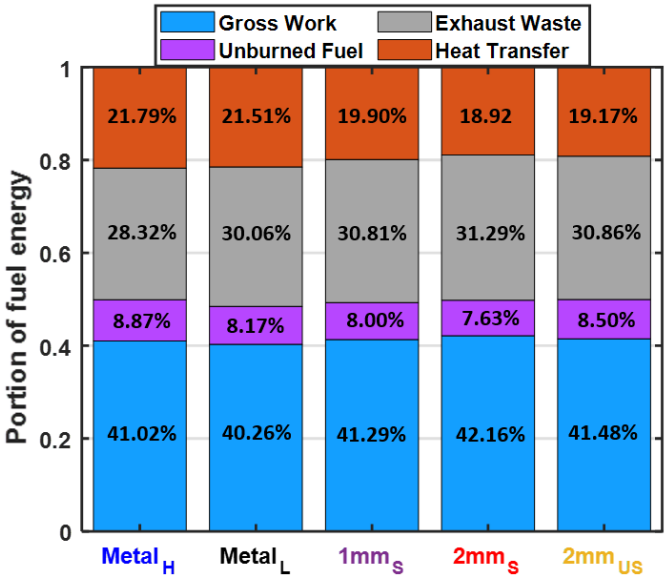

Figure 10: Energy distribution chart for gasoline with the five different pistons at load of 4.6 bar $IMEP_g$. $Metal_H$ is the metal piston with the higher compression ratio and $Metal_L$ is the metal piston with the lower compression ratio.

Emissions – Gasoline

The emissions are shown in Figure 11. The 2mm sealed TBC case has the lowest UHC and CO emissions due to higher surface temperatures which raise the gas temperature of the cold regions near the piston surface. It is interesting to note that the TBCs improve both the UHC and CO emissions, rather than only affecting the UHC emissions. For the 2mm unsealed case, even though the surface temperature is higher than that of the 1mm sealed surface, it has higher UHC emissions, which is assumed to be due to the porous surface storing unburned fuel.

It was hypothesized that the NOx emissions might increase for the TBC cases; however, the results did not break the metal baseline brackets. Therefore, it can be concluded that thick TBC do not negatively impact NO_x emissions.

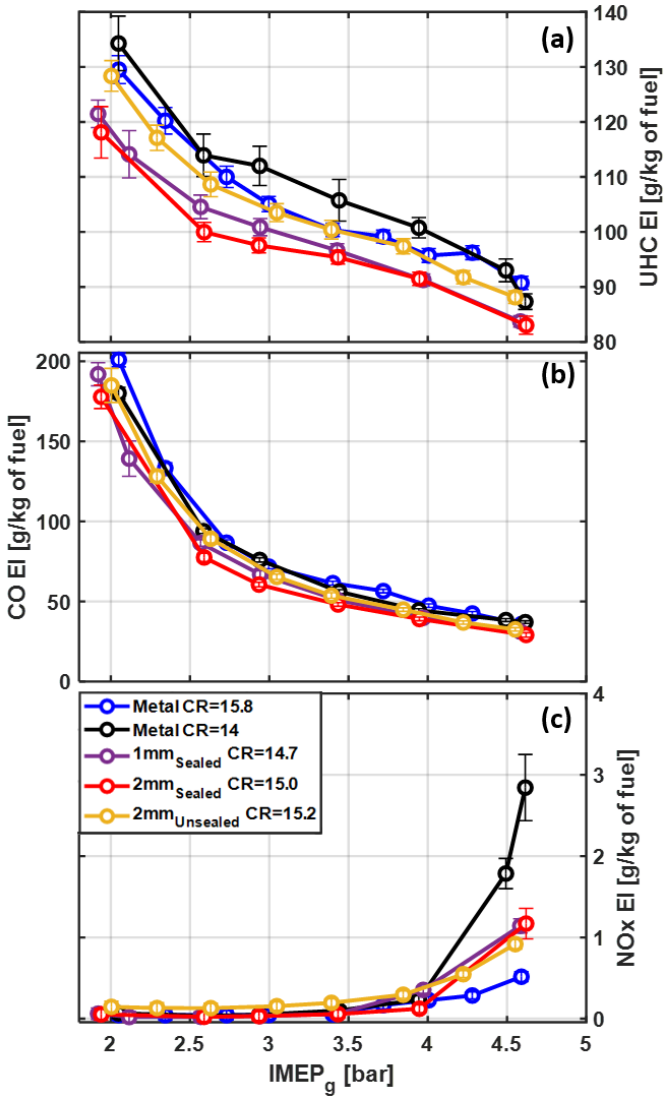

Figure 11: (a) UHC, (b) CO, and (c) NO_x emissions vs. $IMEP_g$

Intake temperature requirement - Gasoline

With conventional combustion modes like SI and diesel combustion, TBC application leads to an intake charge heating penalty, which lowers volumetric efficiency and power density. However, thick TBCs seem to be well-suited to LTC since LTC usually requires higher intake temperatures, especially for fuels with a high-octane number or cooling potential. Figure 12(a) shows the intake temperature with different pistons at different load conditions. For all cases, the temperature requirement reduces as the load increases. Since gasoline is not φ-sensitive at naturally aspirated conditions, this reduced intake temperature requirement is presumably because of the hotter walls and higher residual gas temperatures as load increases. As can be seen, the TBC cases did not break from the brackets of two metal baseline cases; however, the estimated intake temperature for the equivalent compression ratio of 14.9 is shown in green dotted line by taking the average of the two metal cases. Both 2mm cases are able to lower the intake temperature requirement by 15 degrees because the hotter piston surface heats the incoming charge to reach the same temperature after compression to achieve autoignition. The 1mm TBC cases did not show any reduction in intake temperature even compared with the equivalent case, which could be due to the lower CR. The error bars were not applied on this plot because the error for K-type thermocouple is constant at about ±0.4% of the reading value.

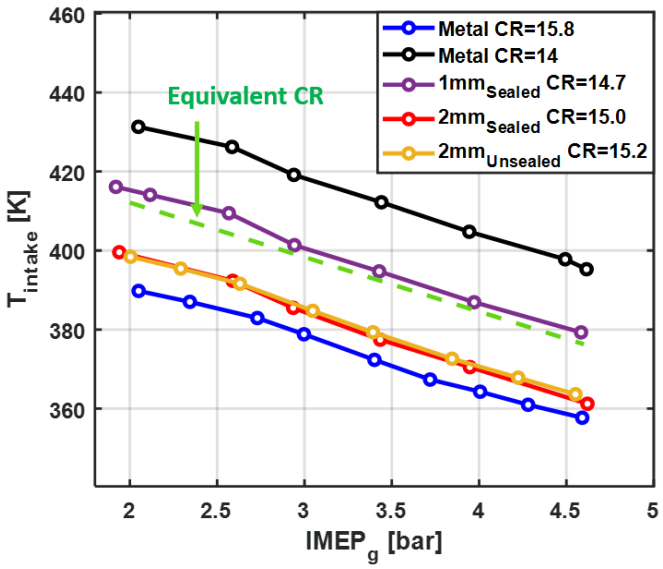

Figure 12: Intake and exhaust temperature vs. $IMEP_g$

Thick TBC with wet ethanol

In this section, similar experiments were conducted with wet ethanol 80 instead of gasoline. The wet ethanol was direct injected at -330 CAD aTDC. The results from one of the metal baseline cases (the higher compression ratio case) and the 2mm sealed TBC case will be compared with the gasoline cases. The comparison is mainly focused on the load range, efficiencies, and intake temperature requirement.

Load range, efficiencies, and energy distribution

– WE80 & gasoline

Figure 13 shows the efficiencies versus the load range of both wet ethanol (dashed lines) and gasoline (solid lines). Since ethanol has a higher octane number, it can be seen that the load range for WE80 is slightly shifted toward higher loads compared to gasoline. For WE80, the 2 mm sealed TBC improves the low-load limit from 2.6 bar IMEPg to 2.2 bar $IMEP_g$, which is an improvement of 15.4%, while the high load limit is approximately constant (5.02 vs. 4.99 bar).

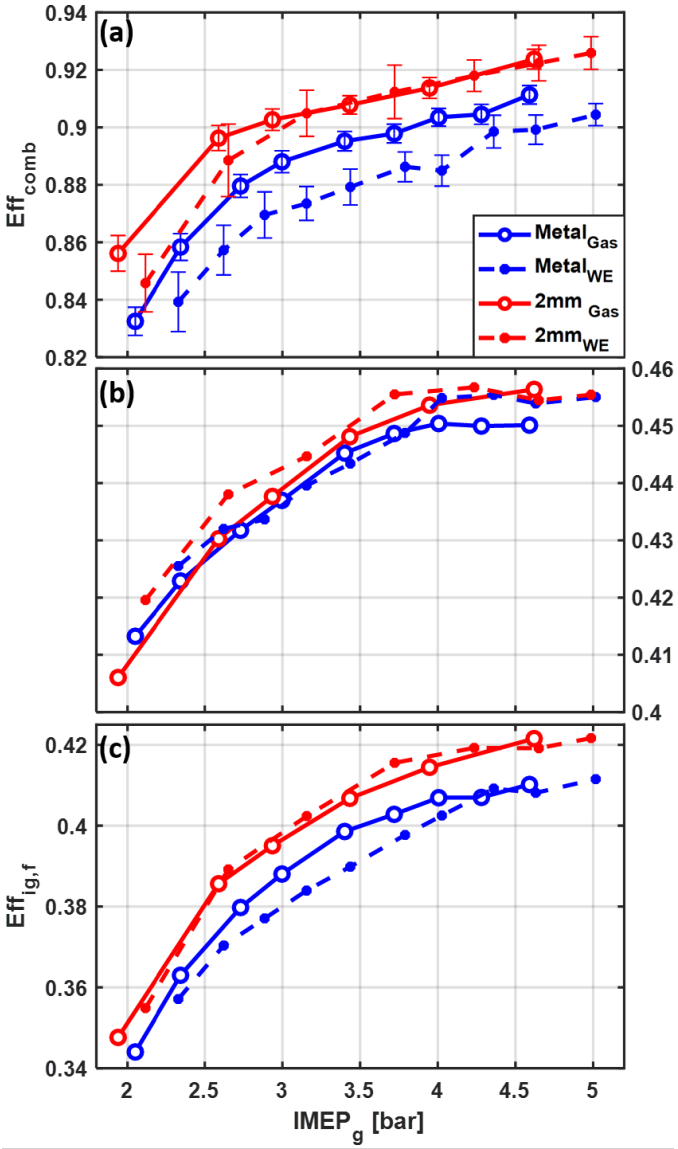

Figure 13: (a) Combustion efficiency, (b) gross indicated thermal efficiency, and (c) gross indicated fuel conversion efficiency vs. $IMEP_g$ for gasoline (solid lines) and wet ethanol (dashed lines)

The combustion efficiency is shown in Figure 13(a). The WE80 metal baseline is generally lower than that of the gasoline. One possible reason is that ethanol has a higher autoignition resistance, which potentially leads to more incomplete combustion from the cold regions. Otherwise, the high cooling potential of WE directly injected into the cylinder and the spray targeting the piston crown during injection might cause poor evaporation and wall wetting on the cold piston surface. The combustion efficiency of WE80 is significantly improved with the 2mm sealed TBC on the piston. At lower loads, gasoline still exhibits higher combustion efficiency because the surface temperature may not be high enough to overcome the evaporative cooling of the WE. But, as the load increases, the surface temperature of the piston increases, which aids evaporation and helps the combustion efficiency of the WE80 case eventually catches up the gasoline case. Overall, the combustion efficiency is increased by up to 1.5 percentage points for WE. The gasoline case experiences most of the combustion efficiency benefits at low loads, while the WE experiences most of its combustion efficiency benefits at mid-to-high load. The emissions data for the WE and gasoline comparison are shown in the Appendix in Figure 18, which agrees well with the illustration above. These combustion efficiency improvements provide evidence of why thick TBCs are well suited to fuels with high evaporative cooling potential.

Thick TBCs provide a similar gross indicated thermal efficiency gain for the WE case as the gasoline case, and the increase in fuel conversion efficiency is higher for the WE due to the larger improvement in combustion efficiency. The plots of thermal efficiency and fuel conversion efficiency did not include error bars because of the clearness of the figure. A version of the fuel conversion efficiency plot that includes error bars is shown in the Appendix in Figure 19.

The energy distribution chart at the load of 4.6 bar for both WE (second highest load for WE) and gasoline (highest load for gasoline) is shown in Figure 14. The distribution structure is similar to Figure 10. For the metal baseline comparison, WE has a slightly higher percentage of work output than gasoline. One of the possible explanations for this is that the air-fuel mixture with WE has a slightly higher ratio of specific heats (γ) than gasoline. Other than that, the distribution for both gasoline and WE are very similar. Reduced heat transfer losses are tangible in both WE and gasoline cases, and the reduction in heat transfer losses for the 2mm sealed piston is about 13.6%. It is important to note that only the piston was coated due to ease in the coating process and the availability of spare piston blanks. However, in a production variant of this concept, the piston, head, and valves would all be coated which would amplify all of the trends shown in this paper.

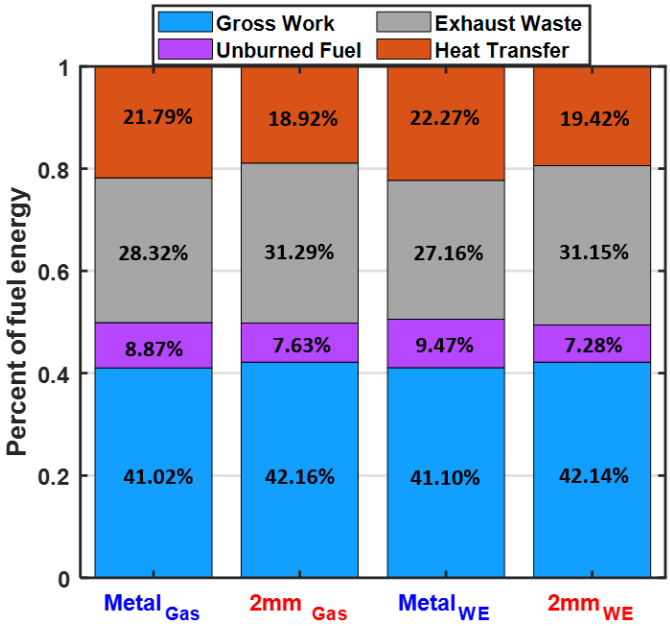

Figure 14:Energy distribution chart for WE80 and gasoline

Intake temperature requirement – WE80 & gasoline

The trends of intake temperature are shown in Figure 15. The intake temperature of all cases decreases as load increases. Since both gasoline and wet ethanol are not φ-sensitive at ambient pressure [19], this decrease in intake temperature is most likely associated with increasing residual gas temperatures and increasing wall temperature. Dec et al. have shown similar trends using iso-octane [45], which is also a single-stage heat release fuel (that is not φ-sensitive) at naturally aspirated conditions.

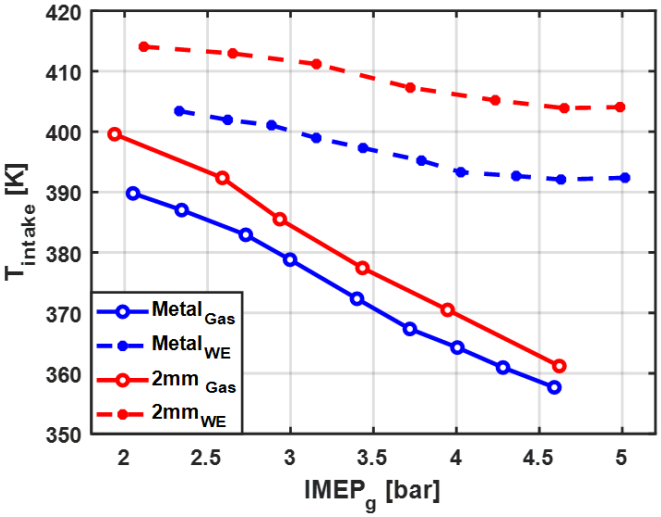

Figure 15: Intake temperature vs. $IMEP_g$

Another interesting trend that can be seen in Figure 15 is that the temperature decreases by about 40 K from the lowest load to the highest load for gasoline – however, it only decreased by about 10 K for WE80. This is because the WE80 has an extremely high evaporative cooling potential. As shown in Figure 16, the cooling potential of WE80 is significantly higher than gasoline (about 6.5 times), and this evaporative cooling increases as the equivalence ratio increases. The high cooling potential needs to be compensated for with intake heating to achieve the autoignition. It is important to note that these results were generated from steady-state operating points. The temperature requirement of the transient operation would be different due to differences in transient wall temperatures, residual properties, and combustion phasings. A similar intake temperature plot as Figure 12 that includes all of the tested pistons for WE80 is shown in the Appendix in Figure 17. The 2mm sealed TBC case is able to decrease the intake temperature requirement by about 10 degrees when compared with the equivalent CR case, but the reduction is not as much as gasoline.

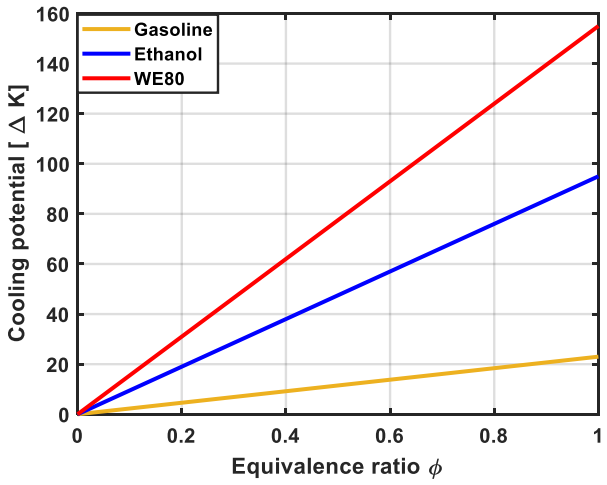

Figure 16:Cooling potential of different fuels

Conclusions

Experiments were conducted on a light duty single-cylinder research engine to investigate the effects of thick thermal barrier coatings on LTC with different fuels. The study mainly focuses on two aspects:

1. The effects of TBC thickness and surface finish (with or without dense sealing layer) on gasoline LTC
2. The potential benefits of TBCs when using an alternative fuel with a high latent heat of vaporization (wet ethanol 80)

In order to achieve a comprehensive investigation, five pistons were tested including:

1. A metal piston baseline at a CR of 15.8
2. A metal piston baseline at a CR of 14
3. A 1mm TBC piston at a CR of 14.7 with a dense sealing layer applied to the surface of the coating
4. A 2mm TBC piston at a CR of 15.2 with a dense sealing layer applied to the surface of the coating
5. A 2mm TBC piston at a CR of 15.0 without the dense sealing layer applied to the top surface of the coating

Two fuels were examined and compared for the pistons listed above: an 87-AKI gasoline and an alternative biofuel with high cooling potential – Wet Ethanol 80. A full load sweep was conducted with each fuel on each piston. The conclusions are as follow:

1. The thick TBCs extend the low load limit by 14.8% with gasoline, and 15.4% with WE80 by improving combustion efficiency. No deterioration of the high load limit was observed.
2. There was no discernible impact by the TBCs on the burn duration or heat release process.
3. The combustion efficiency increases with TBC thickness. The increment is up to 1.5 percentage points with both gasoline and WE80. The gasoline cases experience the most benefits at low load (2 to 3 bar $IMEP_g$), while the WE experiences the most benefits at mid-to-high load (3 to 4.5 bar $IMEP_g$).
4. Higher thermal efficiencies were achieved with TBCs. Increasing the TBC thickness reduces heat transfer losses and improves thermal efficiency. Due to the improved combustion and thermal efficiencies, the fuel conversion efficiency increased by up to 4.3% with WE 80, and 3.8% with gasoline.
5. The dense sealing layer reduces surface porosity and improves UHC emissions and combustion efficiency.
6. With the 2mm TBCs, the intake temperature requirement was reduced by 15 K with gasoline, and 10 K with WE80.
7. No sign of failure was detected after 10-20 hours of engine operation. Photographs of the TBC surfaces (after running in the engine followed by a light cleaning) are shown in the Appendix in Figure 20.

In this study, only the piston was coated, which means that all of the potential benefits such as the efficiency gains, emissions reduction, lower intake temperature requirements, etc. could be amplified if the engine head and valves were also coated.

References

[1]. Assanis, D. and Heywood, J., "Development and Use of a Computer Simulation of the Turbocompounded Diesel System for Engine Performance and Component Heat Transfer Studies," SAE Technical Paper 860329, 1986, https://doi.org/10.4271/860329.

[2]. Wong, V., Bauer, W., Kamo, R., Bryzik, W. et al., "Assessment of Thin Thermal Barrier Coatings for I.C. Engines," SAE Technical Paper 950980, 1995, https://doi.org/10.4271/950980.

[3]. Assanis, D. and Mathur, T., "The Effect of Thin Ceramic Coatings on Spark-Ignition Engine Performance," SAE Technical Paper 900903, 1990, https://doi.org/10.4271/900903.

[4]. Kosaka, H., Wakisaka, Y., Nomura, Y., Hotta, Y. et al., "Concept of "Temperature Swing Heat Insulation" in Combustion Chamber Walls, and Appropriate Thermo-Physical Properties for Heat Insulation Coat," SAE Int. J. Engines 6(1):142-149,

[5]. Moser, S., O'Donnell, R., Hoffman, M., Jordan, E. et al., "Experimental Investigation of Low Cost, Low Thermal Conductivity Thermal Barrier Coating on HCCI Combustion, Efficiency, and Emissions," SAE Technical Paper 2020-01-1140, 2020

[6]. Kamo, R. and Bryzik, W., "Adiabatic Turbocompound Engine Performance Prediction," SAE Technical Paper 780068, 1978, https://doi.org/10.4271/780068.

[7]. Sudhakar, V., "Performance Analysis of Adiabatic Engine," SAE Technical Paper 840431, 1984, https://doi.org/10.4271/840431.

[8]. Kamo, R. and Bryzik, W., "Cummins/TACOM Advanced Adiabatic Engine," SAE Technical Paper 840428, 1984, https://doi.org/10.4271/840428.

[9]. Dec, John E. "Advanced compression-ignition engines—understanding the in-cylinder processes." Proceedings of the combustion institute 32, no. 2 (2009): 2727-2742.

[10]. Reitz, Rolf D. "Directions in internal combustion engine research." Combustion and Flame 1, no. 160 (2013): 1-8.

[11]. Dempsey, Adam B., N. Ryan Walker, Eric Gingrich, and Rolf D. Reitz. "Comparison of low temperature combustion strategies for advanced compression ignition engines with a focus on controllability." Combustion Science and Technology 186, no. 2 (2014): 210-241

[12]. Kuo, Tang-Wei, Barry L. Brown, Paul M. Najt, and James A. Eng. "Valve and fueling strategy for operating a controlled auto-ignition four-stroke internal combustion engine." U.S. Patent 7,021,277, issued April 4, 2006.

[13]. Christensen, M. and Johansson, B., "Supercharged Homogeneous Charge Compression Ignition (HCCI) with Exhaust Gas Recirculation and Pilot Fuel," SAE Technical Paper 2000-01-1835, 2000.

[14]. Olsson, J.-O., Tunestål, P., Haroldsson, G. and Johansson, B., "A Turbo-Charged Dual Fuel HCCI Engine," SAE Technical Paper 2001-01-1896, 2001.

[15]. Saxena, Samveg, and Iván D. Bedoya. "Fundamental phenomena affecting low temperature combustion and HCCI engines, high load limits and strategies for extending these limits." Progress in Energy and Combustion Science 39, no. 5 (2013): 457-488.

[16]. Yan, Ziming, et al. "Investigation Into Reactivity Separation Between Direct Injected and Premixed Fuels in RCCI Combustion Mode." ASME 2019 Internal Combustion Engine Division Fall Technical Conference. American Society of Mechanical Engineers Digital Collection, 2019.

[17]. Reitz, Rolf D., and Ganesh Duraisamy. "Review of high efficiency and clean reactivity controlled compression ignition (RCCI) combustion in internal combustion engines." Progress in Energy and Combustion Science 46 (2015): 12-71.

[18]. Rose, K. D., J. Ariztegui, R. F. Cracknell, T. Dubois, H. D. C. Hamje, L. Pellegrini, D. J. Rickeard, B. Heuser, T. Schnorbus, and A. F. Kolbeck. Exploring a gasoline compression ignition (GCI) engine concept. No. 2013-01-0911. SAE Technical Paper, 2013.

[19]. Dec, J., Yang, Y., and Dronniou, N., "Boosted HCCI - Controlling Pressure-Rise Rates for Performance Improvements using Partial Fuel Stratification with Conventional Gasoline," SAE Int. J. Engines 4(1):1169-1189, 2011, https://doi.org/10.4271/2011-01-0897.

[20]. Yan, Z., Gainey, B., Hariharan, D. and Lawler, B., 2020. Improving the controllability of partial fuel stratification at low boost levels by applying a double late injection strategy. International Journal of Engine Research, p.1468087419896511.

[21]. Lawler, Benjamin, Derek Splitter, James Szybist, and Brian Kaul. "Thermally Stratified Compression Ignition: A new advanced low temperature combustion mode with load flexibility." Applied energy 189 (2017): 122-132.

[22]. Gainey, B., Yan, Z., Gohn, J., Rahimi Boldaji, M. et al., "TSCI with Wet Ethanol: An Investigation of the Effects of Injection Strategy on a Diesel Engine Architecture," SAE Technical Paper 2019-01-1146, 2019, https://doi.org/10.4271/2019-01-1146.

[23]. Dec, J. and Sjöberg, M., "A Parametric Study of HCCI Combustion - the Sources of Emissions at Low Loads and the Effects of GDI Fuel Injection," SAE Technical Paper 2003-01-0752, 2003, https://doi.org/10.4271/2003-01-0752.

[24]. Flowers, D., Aceves, S., and Frias, J., "Improving Ethanol Life Cycle Energy Efficiency by Direct Utilization of Wet Ethanol in HCCI Engines," SAE Technical Paper 2007-01-1867, 2007, https://doi.org/10.4271/2007-01-1867.

[25]. Farrell, Alexander E., Richard J. Plevin, Brian T. Turner, Andrew D. Jones, Michael O'hare, and Daniel M. Kammen. "Ethanol can contribute to energy and environmental goals." Science 311, no. 5760 (2006): 506-508.

[26]. Saffy, Howard A., William F. Northrop, David B. Kittelson, and Adam M. Boies. "Energy, carbon dioxide and water use implications of hydrous ethanol production." Energy conversion and management 105 (2015): 900-907.

[27]. Gainey, B., Gohn, J., Yan, Z., Malik, K. et al., "HCCI with Wet Ethanol: Investigating the Charge Cooling Effect of a High Latent Heat of Vaporization Fuel in LTC," SAE Technical Paper 2019-24-0024, 2019.

[28]. Gainey, B., Hariharan, D., Yan, Z., Zilg, S., Rahimi Boldaji, M., & Lawler, B. (2018). A split injection of wet ethanol to enable thermally stratified compression ignition. International Journal of Engine Research, 1468087418810587.

[29]. Yan, Z., Gainey, B., Gohn, J., Hariharan, D. et al., "The Effects of Thick Thermal Barrier Coatings on Low-Temperature Combustion," SAE Technical Paper 2020-01-0275, 2020.

[30]. Benajes, Jesús, Antonio García, José Manuel Pastor, and Javier Monsalve-Serrano. "Effects of piston bowl geometry on Reactivity Controlled Compression Ignition heat transfer and combustion losses at different engine loads." Energy 98 (2016): 64-77.

[31]. Chang, J., Güralp, O., Filipi, Z., Assanis, D. et al., "New Heat Transfer Correlation for an HCCI Engine Derived from Measurements of Instantaneous Surface Heat Flux," SAE Technical Paper 2004-01-2996, 2004, https://doi.org/10.4271/2004-01-2996.

[32]. Gainey, B., Longtin, J., and Lawler, B., "A Guide to Uncertainty Quantification for Experimental Engine Research and Heat Release Analysis," SAE Int. J. Engines 12(5):509-523, 2019, https://doi.org/10.4271/03-12-05-0033.

[33]. Beardsley, M. Brad, Darrell Socie, Ed Redja, and Christopher Berndt. Thick Thermal Barrier Coatings (TTBCs) for Low Emission, High Efficiency Diesel Engine Components. No. DOE/OR/22580-1. Caterpillar Inc., PO Box 1875, Peoria, IL 61656-1875, 2006.

[34]. Hutchinson, J. W., and A. G. Evans. "On the delamination of thermal barrier coatings in a thermal gradient." Surface and Coatings Technology 149, no. 2-3 (2002): 179-184.
[35]. Sampath, S., W. C. Smith, T. J. Jewett, and Hwan Kim. "Synthesis and characterization of grading profiles in plasma sprayed NiCrAlY-zirconia FGMs." In Materials science forum, vol. 308, pp. 383-388. Trans Tech Publications, 1999.
[36]. Srinivasan, V., M. Friis, A. Vaidya, T. Streibl, and S. Sampath. "Particle injection in direct current air plasma spray: Salient observations and optimization strategies." Plasma Chemistry and Plasma Processing 27, no. 5 (2007): 609-623.
[37]. Vaidya, A., V. Srinivasan, T. Streibl, M. Friis, W. Chi, and S. Sampath. "Process maps for plasma spraying of yttria-stabilized zirconia: An integrated approach to design, optimization and reliability." Materials Science and Engineering: A 497, no. 1-2 (2008): 239-253.
[38]. Finot, M., S. Suresh, C. Bull, and S. Sampath. "Curvature changes during thermal cycling of a compositionally graded Ni Al2O3 multi-layered material." Materials
[39]. Lawler B, Mamalis S, Joshi S, Lacey J, Guralp O, Najt P and Filipi Z. Effect of operating conditions on thermal stratification and heat release in a homogeneous charge compression ignition engine. Appl Therm Eng 2017; 112: 392–402
[40]. Dronniou, N. and Dec, J., "Investigating the Development of Thermal Stratification from the Near-Wall Regions to the Bulk-Gas in an HCCI Engine with Planar Imaging Thermometry," SAE Int. J. Engines 5(3):1046-1074, 2012, https://doi.org/10.4271/2012-01-1111.
[41]. Heywood, John B. Internal Combustion Engine Fundamentals. New York: McGraw-Hill Education, 2018.
[42]. Sjöberg, M. and Dec, J., "Combined Effects of Fuel-Type and Engine Speed on Intake Temperature Requirements and Completeness of Bulk-Gas Reactions for HCCI Combustion," SAE Technical Paper 2003-01-3173, 2003, https://doi.org/10.4271/2003-01-3173.
[43]. Tree, D., Wiczynski, P., and Yonushonis, T., "Experimental Results on the Effect of Piston Surface Roughness and Porosity on Diesel Engine Combustion," SAE Technical Paper 960036, 1996, https://doi.org/10.4271/960036 -Effects of Engine Variables," SAE Technical Paper 2004-01-1971, 2004, https://doi.org/10.4271/2004-01-1971.
[44]. Hoffman, Mark A., Benjamin J. Lawler, Orgun A. Güralp, Paul M. Najt, and Zoran S. Filipi. "The impact of a magnesium zirconate thermal barrier coating on homogeneous charge compression ignition operational variability and the formation of combustion chamber deposits." International Journal of Engine Research 16, no. 8 (2015): 968-981.
[45]. Dec, J. and Sjöberg, M., "Isolating the Effects of Fuel Chemistry on Combustion Phasing in an HCCI Engine and the Potential of Fuel Stratification for Ignition Control," SAE Technical Paper 2004-01-0557, 2004, https://doi.org/10.4271/2004-01-0557.

Contact Information

Ziming Yan
zimingy@clemson.edu
yanziminga@gmail.com
Benjamin Lawler
bjlawle@clemson.edu

Definitions/Abbreviations

aTDC	after top dead center
APS	atmospheric plasma spray
CAD	crank angle degree
CA50	crank angle of 50% mass fraction burned
CCD	combustion chamber deposit
CO	carbon monoxide
COV	coefficient of variation
CR	compression ratio
CTE	coefficient of thermal expansion
DI	direct injected
EGR	external-cooled exhaust gas recirculation
GHRR	gross heat release rate
HCCI	homogeneous charge compression ignition
HOF	latent heat of vaporization
$IMEP_n$	net indicated effective mean pressure
IVO	intake valve open
LTC	low-temperature combustion
NHRR	net heat release rate
NLPM	Normal liter per minute
NO_x	nitrogen oxides
OEM	original equipment manufacturer
OHC	oxygenated hydrocarbon
PPRR	peak pressure rise rate
RCCI	reactivity-controlled compression ignition
SOI	start of injection
SI	spark ignition
TBCs	thermal barrier coatings
TSCI	thermally stratified compression ignition
UHC	unburned hydrocarbon
YSZ	yttria-stabilized zirconia

Appendix:

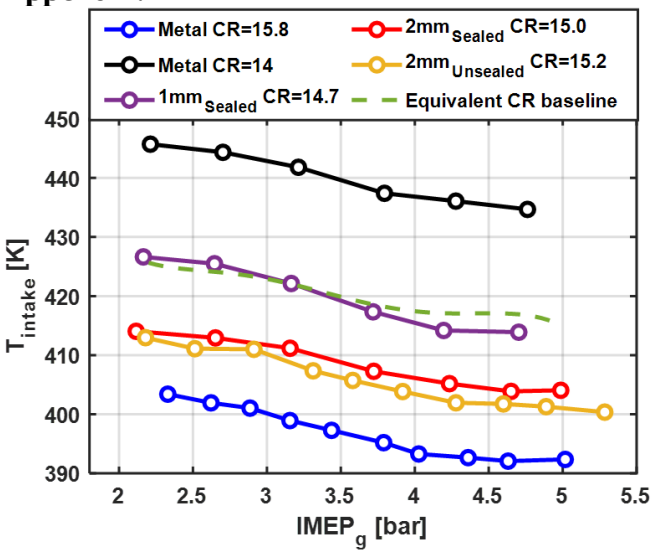

Figure 17: Intake and exhaust temperature vs. $IMEP_g$ (Wet Ethanol 80)

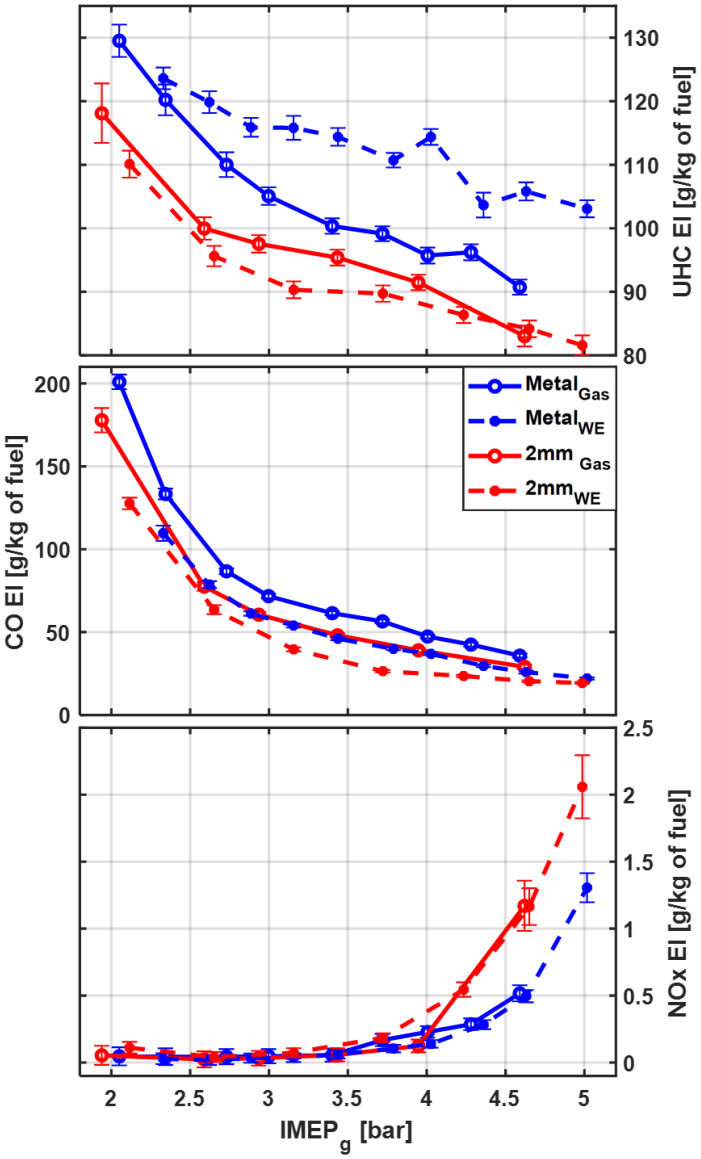

Figure 18: (a) UHC, (b) CO, and (c) NO_x emissions vs. $IMEP_g$ for gasoline (solid lines) and wet ethanol (dashed lines)

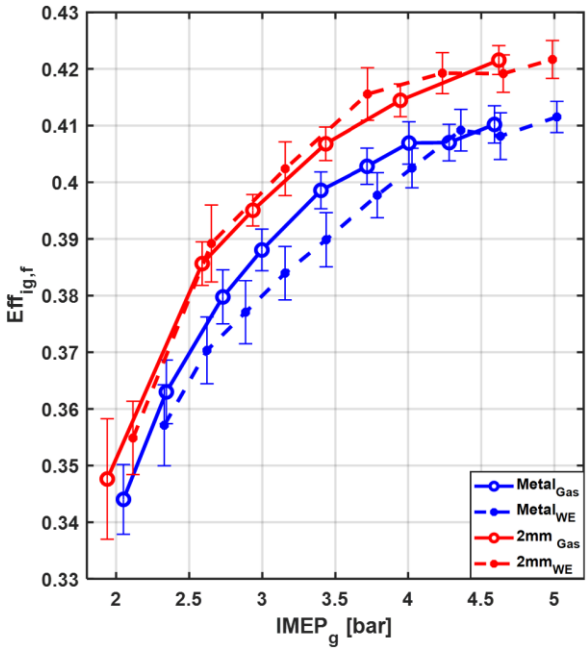

Figure 19: Fuel conversion efficiency vs. $IMEP_g$ for gasoline (solid lines) and wet ethanol (dashed lines)

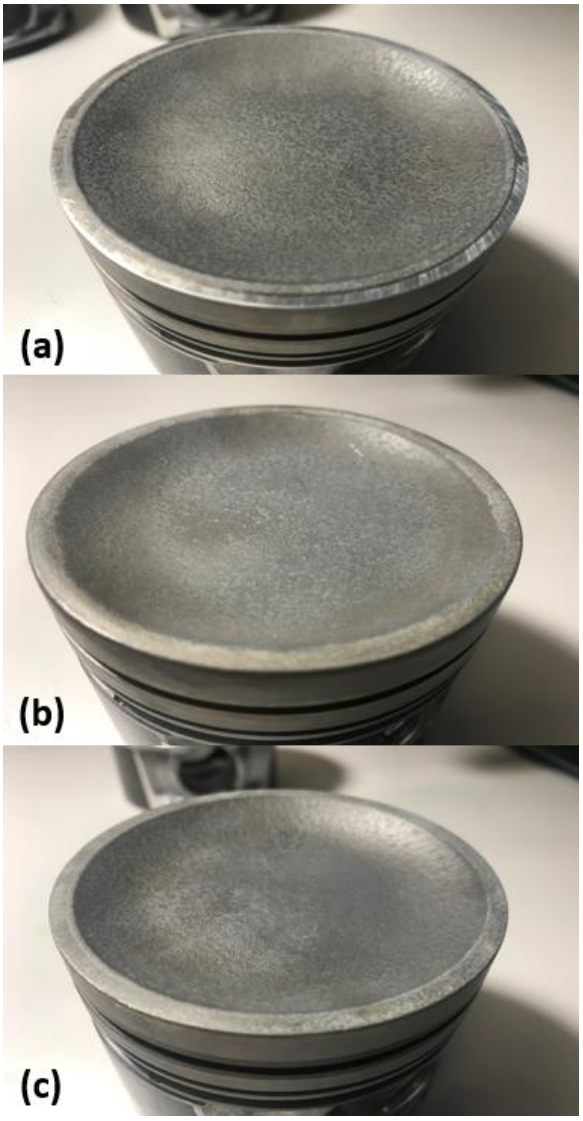

Figure 20: Photographs of the pistons after 10-20 hours of testing. (a) 1mm sealed, (b) 2 mm sealed, (c) 2 mm unsealed